



Total photosynthetic biomass record between 9400 and 2200 BP and its link to temperature changes at a High Arctic site near Ny-Ålesund, Svalbard

Zhongkang Yang¹ · Jianjun Wang² · Linxi Yuan³ · Wenhan Cheng¹ · Yuhong Wang¹ · Zhouqing Xie¹ · Liguang Sun¹

Received: 20 July 2018 / Revised: 17 March 2019 / Accepted: 18 March 2019 / Published online: 5 April 2019
© Springer-Verlag GmbH Germany, part of Springer Nature 2019

Abstract

Changes in vegetation biomass have a great impact on many aspects of the Arctic ecosystem, and historical variations of biomass in Svalbard during the Holocene remain poorly understood. In this study, we collected a palaeo-notch sediment profile in Ny-Ålesund, Svalbard, performed organic biomarker and geochemical analysis on the sediments, reconstructed the photosynthetic biomass record during the interval of 9400–2200 BP, and examined the relationship between the photosynthetic biomass changes and Holocene temperature records in the Arctic region. The photosynthetic biomass production in Ny-Ålesund experienced four development periods. It rose steadily at the beginning of the Holocene and became stabilized at a high level during the Holocene thermal maximum. However, the photosynthetic biomass dropped sharply during the mid-Holocene transition. After that, it showed a small peak during the interval of 3000–2500 BP. The historical photosynthetic biomass record is in good agreement with the temperature records: the photosynthetic biomass production increases during warmer periods, and vice versa. Therefore, temperature is likely the driving factor controlling the photosynthetic biomass production. This study improves our understanding of the terrestrial ecosystem and its responses to climate change in the Arctic.

Keywords Holocene · Phytol · Bio-elements · Photosynthetic biomass · Svalbard

Electronic supplementary material The online version of this article (<https://doi.org/10.1007/s00300-019-02493-5>) contains supplementary material, which is available to authorized users.

✉ Zhouqing Xie
zqxie@ustc.edu.cn

✉ Liguang Sun
slg@ustc.edu.cn

¹ Anhui Province Key Laboratory of Polar Environment and Global Change, School of Earth and Space Sciences, University of Science and Technology of China, Hefei 230026, China

² Key Laboratory of Global Change and Marine-Atmospheric Chemistry, Third Institute of Oceanography, State Oceanic Administration, Xiamen 361005, China

³ Advanced Lab for Selenium and Human Health, Suzhou Institute for Advanced Study, University of Science and Technology of China, Suzhou 215123, China

Introduction

The Late Weichselian ice sheet covered Svalbard and the entire Barents Sea during the Last Glacial Maximum (Landvik et al. 1998). Around 15,000 BP, the Barents ice sheet started to melt (Svendsen et al. 1996; Landvik et al. 1998) and the Svalbard shelves were largely deglaciated around 12,000 BP (Landvik et al. 1998). From then on, the islands gradually appeared and seawater started to pour into the fjords with the retreat of glaciers at about 10,000 BP (Lehman and Forman 1992; Mangerud et al. 1992; Forman et al. 2004). The Kongsfjorden was completely deglaciated by 9440 ± 130 BP (Lehman and Forman 1992; Forman et al. 2004).

The Svalbard Archipelago is located between the Arctic Ocean and the North Atlantic Ocean. The thermohaline circulation and North Atlantic Oscillation (NAO), the most well-known coupled ocean–atmospheric oscillations in the North Atlantic region, had a great impact on the Holocene climate of Svalbard. An arm of the thermohaline circulation flows northwards along western Svalbard and produces a

polar maritime climate along the western regions (van der Bilt et al. 2016; Yang et al. 2017). In addition, the temperature in the Arctic region is warming at a speed twice the global average, a phenomenon known as Arctic amplification (Cohen et al. 2014). Thus, all these facts make Svalbard among the most sensitive ecosystems to climatic changes (van der Bilt et al. 2016; Yang et al. 2017). A study of a marine sediment core collected on the western shelf of Svalbard outside Kongsfjorden indicated that the sea surface temperature began to increase from ~9600 BP, reached a Holocene thermal maximum during the interval 9000–5500 BP, and declined to the lowest levels between 5000 and 2000 years BP (Rasmussen et al. 2014), which is in line with the other Svalbard shelf records (Chistyakova et al. 2010; Risebrobakken et al. 2010). Although many climate reconstructions have been performed to investigate the temperature variations (Isaksson et al. 2003; Rozema et al. 2006; Jessen et al. 2010; Divine et al. 2011; Müller et al. 2012; Alsos et al. 2016; van der Bilt et al. 2016; Werner et al. 2016) and glacier activities (Landvik et al. 1998; Reusche et al. 2014; Røthe et al. 2015; van der Bilt et al. 2015) in Svalbard, changes of biomass on millennial timescales in Svalbard during the Holocene remain poorly understood. Concerning the fact that vegetation biomass changes have a great impact on many aspects of Arctic ecosystem including wildlife, hydrological cycles and the status of the permafrost (Walker et al. 2005), reconstruction of Holocene photosynthetic biomass production variations and understanding the response to climatic changes are very important.

As organic biomarkers are more resistant to degradation in cold environments and may be preserved for thousands of years (Ogura et al. 1990; Cheng et al. 2016), they have been successfully used to trace vegetation history and penguin populations in the Antarctic (Wang et al. 2007; Huang et al. 2010). Phytol is an organic biomarker, which is mainly derived from the isoprenoid side-chain of chlorophyll-*a* in phytoplankton and terrestrial plants, and it is thus regarded as a good indicator of photosynthetic biomass (Boon et al. 1996; Bechtel and Schubert 2009). Muraoka et al. (2008) studied the photosynthetic characteristics and biomass distribution of the dominant vascular plant species in Ny-Ålesund, Svalbard and found that the net primary production increased with the successional status. Thus the net primary production in Ny-Ålesund, Svalbard reflects the photosynthetic capacity and biomass distribution (Muraoka et al. 2008). Since the phytol in the lacustrine sediment is mainly derived from plant detritus and photosynthetic algae, the phytol contents can be used as a paleoecological proxy of reconstructing historical records of photosynthetic biomass changes. In addition, inorganic bio-elements have been identified as an important geochemical marker to indicate the input of specific material sources, such as seabird populations (Sun et al. 2000; Liu et al. 2006; Xu et al. 2011),

and one advantage of using bio-elements as a paleoclimatic proxy is their stability after deposition. Therefore, bio-elements could be used as an auxiliary proxy of biomass reconstructions for some lacustrine sediments.

In the present study, we reconstructed the photosynthetic biomass record during the interval of 9400–2200 BP at a High Arctic site near Ny-Ålesund, Svalbard, utilizing the phytol contents and bio-elements of a palaeo-notch sediment, and examined the relationship between the photosynthetic biomass changes and Holocene temperature variations in the Arctic region.

Regional setting

Svalbard (74°–81°N, 10°–35°E) is a High Arctic Archipelago located between the Arctic Ocean and the North Atlantic Ocean. It is composed of three large islands (Spitsbergen, Nordaustlandet, Edgeoya) and dozens of small islands. The total area of Svalbard is 62,700 km², 60% of which is covered by glaciers; the permafrost is up to 500 m thick. Because the West Spitsbergen Current flows northwards along western Svalbard, the climate in the western part of Svalbard is generally warmer than other places at corresponding latitudes.

Ny-Ålesund (78°55'N, 11°56' E) is located on the west coast of Spitsbergen (Fig. 1). The meteorological station at Ny-Ålesund in 1981–2010 recorded an average annual temperature of –5.2 °C and an average annual precipitation of 427 mm (Førland et al. 2011). Most precipitation is related to cyclonic systems and occurs in the autumn and winter months (Førland et al. 2011). The atmospheric and oceanic circulation patterns over Svalbard have a great impact on the regional climate variations. According to the circumpolar Arctic vegetation map (Walker et al. 2005), vegetation in the non-glacier areas of Svalbard is a mix of prostrate dwarf-shrub tundras (14%), cryptogams, forb barrens (10%), and wetlands (8%). The tundra plants in the study area comprise various moss and vascular plant species, and several common tundra plants (*Dicranum angustum*, *Puccinellia phryganodes*, *Salix polaris* and *Saxifraga oppositifolia*) could be found near the sampling site (Yuan et al. 2010).

Materials and methods

Sample collection

A 118-cm-long undisturbed sediment profile was collected from a palaeo-notch on the first terrace (the lowest terrace) of Ny-Ålesund, Svalbard, during an Arctic expedition in the summer of 2004 (Fig. 1) and labeled YN. The notches are common on limestone coasts and are undercuttings or

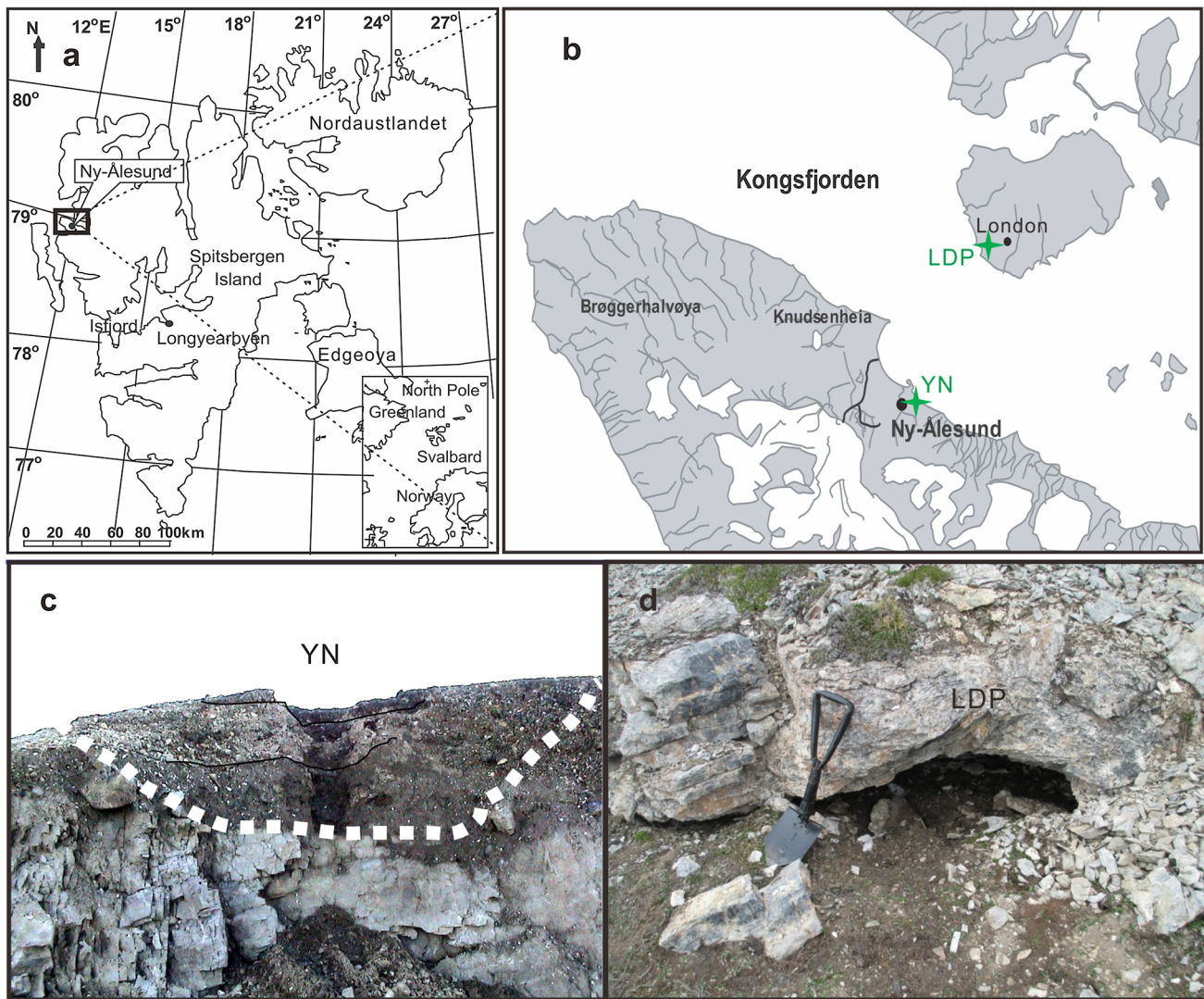


Fig. 1 The Svalbard Archipelago (a) showing the Yn and LDP sampling sites in Ny-Ålesund (b), the palaeo-notch YN (c) and the palaeo-notch LDP (d)

indentations that are carved by ocean waves near sea level. The limestone bedrock in the study area became exposed after deglaciation and eroded by ocean waves to form a rock notch (palaeo-notch in this study). Then, the rock notch was exposed after the terrace lifted up and began to receive deposits. This palaeo-notch opens towards the sea and has a smooth bottom. The sampling site ($78^{\circ}55.6'N$, $11^{\circ}56.4'E$) is about 3 m away from the ocean and 3.5 m above sea level. According to lithological characteristics and color differences, the sediment profile could be divided into three layers: 0–10 cm, 10–70 cm, and 70–118 cm. Layer 0–10 cm was sectioned at 2-cm intervals and labeled YN-1–YN-5. Layer 10–70 cm comprises many gravels and was thus sectioned at 10-cm intervals and labeled YN-6–YN-11. Layer 70–118 cm was sectioned at 2-cm intervals and labeled YN-12–YN-35. A 36-cm-long palaeo-notch sediment profile (LDP) (Yang

et al. 2018a) collected from Blomstrandhalvøya Island, about 5 km from Ny-Ålesund was used for chronological correction in this study (Fig. 1). All the samples were frozen and brought back to the laboratory at the University of Science and Technology of China for analysis.

Analytical methods

All the air-dried samples were pulverized into powder with a mortar and pestle, and then sieved through a 200-mesh sieve.

For analysis of phytol, *n*-alkanols and *n*C₁₈ fatty acids, the samples were Soxhlet-extracted with 2:1 dichloromethane/methanol for 72 h. The extracts were concentrated by rotary evaporation and then saponified using 0.5 mol L^{-1} KOH/MeOH. Neutral lipids were partitioned out of the basic solution with hexane. The pH of the saponified extract was then

brought to a value of 2 with 6 N HCl, and acidic lipids were extracted with 20% methylene chloride in hexane. Acidic lipids were placed in the presence of anhydrous Na₂SO₄ overnight in order to remove traces of water. Neutral lipids were further separated on 5% deactivated silica gel column chromatography using solvents of increasing polarity from hexane through methylene chloride. The fractions containing hydrocarbons (eluted with hexane) and *n*-alkanols/sterols (eluted with methylene chloride) were collected separately. The alcohols and acids fraction was treated with BSTFA (*N,O*-bis-trimethylsilyltrifluoroacetamide) to form trimethylsilyl-ether derivatives. The silylated extract fractions were analyzed on an HP 5890 GC–MS system with a DB-5MS (50 m × 0.32 mm and 0.25-μm film thickness) capillary column (J&W). Helium was used as the carrier gas. The MS was operated in electron impact mode at 70 eV ionization energy. The GC oven was programmed as follows: hold 2 min at 60 °C, increase to 150 °C at 10 °C/min, increase to 300 °C at 2.5 °C/min, hold 30 min at 300 °C. The results were monitored by analyzing the Standard Reference Material (SRM: cholesterol-2,2,3,4,4,6-d6) and the data were acquired in the full scan mode and processed with the Chemstation data system.

A total of 16 major and trace elements, Cu, Zn, Pb, Ni, Mn, P₂O₅, Cd, F, Hg, Se, K₂O, Na₂O, CaO, MgO, Fe and Al₂O₃, were measured for all the samples. The detailed analytical methods have been described by Liu et al. (2005). For chemical analysis, the precision and accuracy were monitored by analyzing sediment SRMs in every batch of analysis, and the analytical values for the major elements and trace elements are within ±0.5% and ±5% of the certified ones, respectively. Total organic carbon (TOC) content was determined using the chemical volumetric method (Sun et al. 2004). Total nitrogen (TN) content was measured using the Kjeldahl digestion method. Grain size of all 35 samples in profile YN was analyzed using a LS230 laser diffraction particle size analyzer (Beckman Coulter).

Statistical analysis

R-mode cluster analysis and principal component analysis (PCA) were carried out on 13 geochemical proxies for Layer 70–118 cm from the palaeo-notch sediment YN using the software program SPSS 25.0. The main advantage of using bio-elements as climate proxy is their stability after deposition. However, inorganic bio-elements can be remarkably influenced by weathering soil and other background inputs (Sun et al. 2000; Liu et al. 2005, 2006). Because chemical weathering is an important material source in the palaeo-notch sediment (Yang et al. 2018a), chemical weathering elements, K, Na, Fe, Al and Mg, were excluded from the analysis in order to determine the main material source except for chemical weathering. R-mode cluster analysis was

performed to determine the bio-elements of total biomass production and PCA was performed to obtain the scores of PC1 (the first principal component), which was used as the proxy of the main material source input.

Results

Lithological characteristics and radiocarbon dating results

According to the chemical and physical characters, such as components, colors, and grain size, coupled with field observations, three layers of the sediment profile were identified (Fig. 2):

0–10 cm: a gray-black clay layer, its color was darker than the other layers, and it was rich in organic matter content as supported by the TOC and TN contents. The high organic matter content is likely related to rapid warming and anthropogenic impacts in recent decades. This layer also contained some gravels with diameters varying from 1 mm to 1 cm.

10–70 cm: a brown gravel layer. There were a large number of subangular and poorly oriented gravels of diameter between 3 mm and 5 cm. Ice scrapes could be observed on some gravels. This layer was poorly sorted and its mean grain size was notably larger than other layers.

70–118 cm: a brown clay layer with shell remains. This layer had a great variation of color from brown-yellow at the top to brown-black, yellow-green and brown-red at the bottom.

The sedimentary environment for the three layers in sediment profile YN was significantly different from each other. Since Layer 10–70 cm was the glacial deposit caused by glacier activities (unpublished data), we focused on the 70- to 118-cm layer in order to reconstruct photosynthetic biomass changes of Ny-Ålesund recorded in this layer.

For chronological analysis, we performed radiocarbon dating on 4 samples at the Keck Carbon Cycle AMS Facility, Earth System Science Department, UC Irvine, USA, and 5 samples at the Center for Applied Isotope Studies, University of Georgia, USA (Table 1). The radiocarbon dates were then calibrated into calendar years before present (BP) by the calibration curve, IntCal13 (Reimer et al. 2013).

Organic biomarkers

Phytol derives from the side-chain of chlorophyll and represents the total amount of photosynthetic biomass production (Rontani and Volkman 2003). The phytol contents of Layer 70–118 cm in sediment profile YN ranged from 0.1

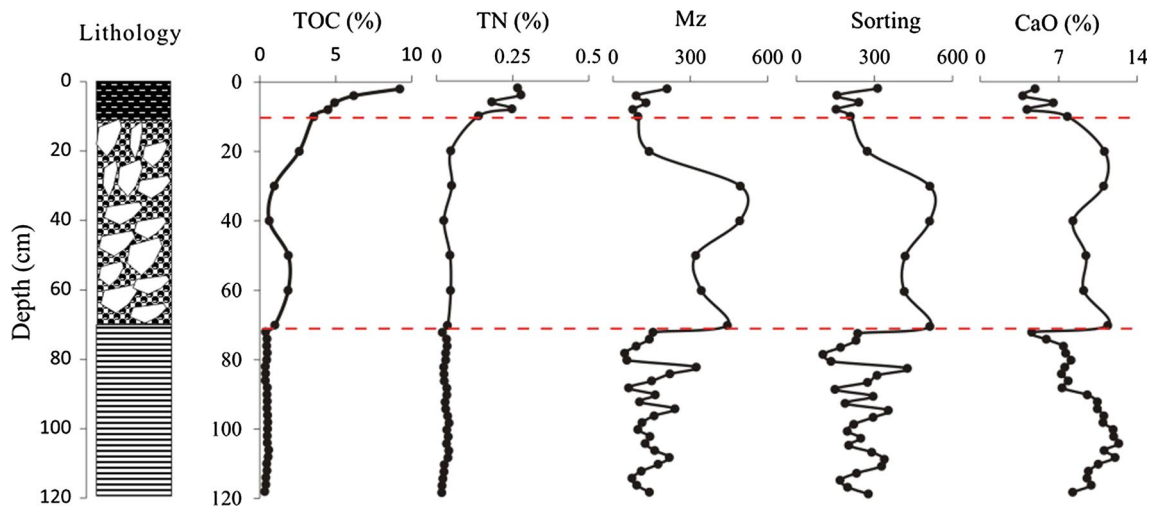


Fig. 2 Sediment lithology for palaeo-notch sediment YN and down-core variation profiles of total organic carbon (TOC), total nitrogen (TN), mean grain size, sorting coefficient and CaO content in YN

Table 1 AMS ^{14}C dates and the calibrated ages of the palaeo-notch sediment YN

Sample ID	Lab code	Depth (cm)	Material	^{14}C age (BP)	Calibrated age (cal. a BP) (σ)	Calibrated age (cal. a BP) (2σ)
YN-14	50296	76	Bulk sediment	$27,820 \pm 220$	31,304–31,775	31,162–32,263
YN-20	50297	88	Bulk sediment	$24,440 \pm 160$	28,305–28,679	28,071–28,814
YN-26	50298	100	Bulk sediment	$28,690 \pm 190$	32,483–33,158	32,023–33,420
YN-31	50299	110	Bulk sediment	$31,210 \pm 330$	34,770–35,438	34,495–35,839
YN-15	19048	78	Bulk sediment	9890 ± 30	11,241–11,292	11,227–11,356
YN-19	19049	86	Bulk sediment	$12,200 \pm 30$	14,036–14,144	13,983–14,204
YN-25	19050	98	Bulk sediment	$12,080 \pm 30$	13,843–14,001	13,786–14,068
YN-28	19051	104	Bulk sediment	$12,550 \pm 30$	14,769–15,016	14,655–15,114
YN-34	19052	116	Bulk sediment	$12,300 \pm 30$	14,121–14,279	14,074–14,460

to $1.7 \mu\text{g g}^{-1}$, with an average value of $0.9 \mu\text{g g}^{-1}$, and the vertical variation pattern of phytol concentrations is shown in Fig. 3. The phytol contents were initially at low levels, started to rise steadily, maintained a relatively high level with a peak around 105 cm and then displayed a rapid decrease and large fluctuation above 90 cm. Overall, the vertical profile of phytol contents was consistent with the TOC profile (Fig. 3).

Fatty alkanols are derived from the epicuticular waxes of vegetation and could be used to distinguish different types of vegetation (Wang et al. 2007). In general, the *n*-alkanol distribution is dominated by C_{16} – C_{22} for algae, and by C_{26} , C_{28} and C_{30} for terrestrial plants (Meyers 2003; Wang et al. 2007). In the present study, we chose C_{18} – C_{20} and C_{28} – C_{30} *n*-alkanol as the representative biomarkers for algae and terrestrial plants, respectively. As shown in Fig. 3, the content of *n*C18-ol was significantly higher than that of *n*C20-ol. In addition, the vertical profiles of

*n*C18-ol, *n*C28-ol and *n*C30-ol exhibited high levels below 85 cm and then decreased to very low levels from 85 to 70 cm.

Fatty acids are ubiquitously found in lacustrine and marine sediments. *n*C₁₈ fatty acids are an important composition of the cell membranes and the proportion of unsaturated acids in organisms increases under cold environment conditions (Meyers 2003). The changes in the ratio of sedimentary *n*C_{18:2} and *n*C_{18:0} has been used to reconstruct the palaeotemperature of Lake Biwa, Japan (Kawamura and Ishiwatari 1981). High $\text{C}_{18:2}/\text{C}_{18:0}$ ratios correspond to cold climate conditions, and vice versa. Therefore, the $\text{C}_{18:2}/\text{C}_{18:0}$ ratio could be applied as a good proxy of palaeotemperature. The vertical profiles of the $\text{C}_{18:2}/\text{C}_{18:0}$ ratio for the palaeo-notch sediment YN exhibited very low values (warm climate) in the interval 85–118 cm and high values (cold climate) from 85 to 70 cm (Fig. 3).

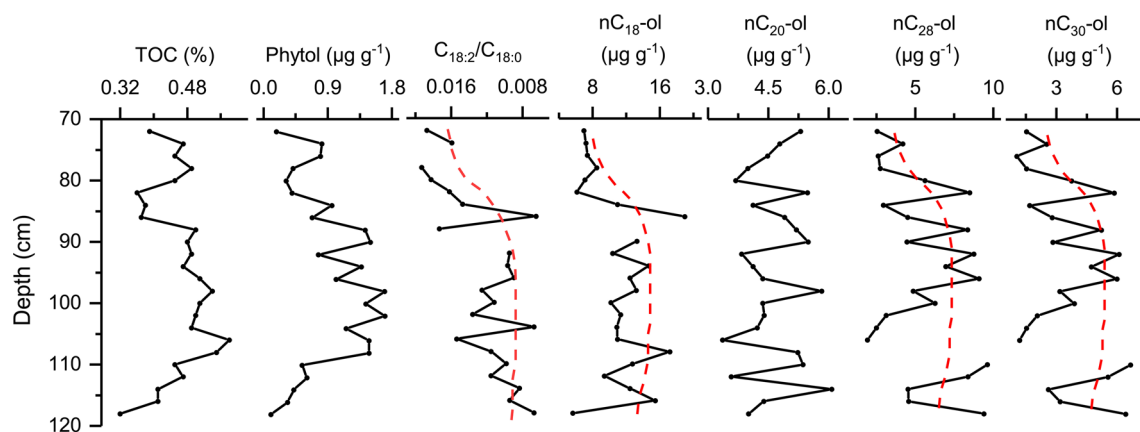


Fig. 3 Down-core variation profiles of TOC, phytol contents, $C_{18:2}/C_{18:0}$ fatty acids ratios and *n*-alkanols contents in the palaeo-notch sediment YN (70–118 cm)

Elemental concentrations

The TOC and TN contents of the sediment profile YN have been published in Yuan et al. (2010). The concentration-versus-depth profiles of typical elements in Layer 70–118 cm are plotted in Fig. 4 and show substantial fluctuations. Elements Se, Pb, CaO and Zn had vertical variation patterns very similar to those of phytol contents, TOC

and TN. The concentrations all rose from very low levels at the beginning and reached peak values between 100 and 110 cm. The major element oxides, Al_2O_3 , K_2O , Fe_2O_3 and MgO , had very consistent change patterns: their levels tended to fluctuate within a very small range below 90 cm and showed dramatic changes at the depth of 80–90 cm. However, the elements/oxides, Ni, Cu, Mn, P_2O_5 , Hg, Cd, F and Na_2O , showed frequent variations of complex patterns with inconsistent peaks and troughs.

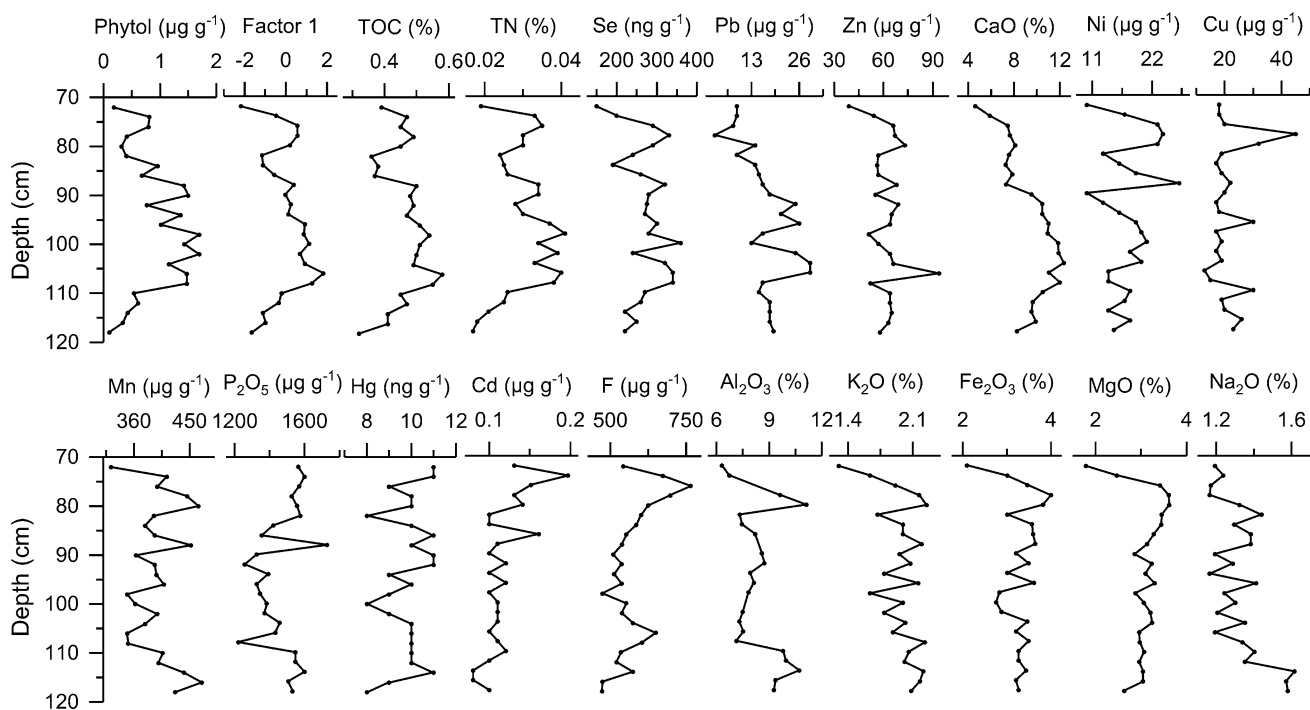


Fig. 4 Down-core variation profiles of the elements/oxides and phytol contents in the palaeo-notch sediment YN as well as the variation of loadings for factor 1 (PC1)

Statistical analysis results

R-mode cluster analysis for 13 geochemical proxies from the palaeo-notch sediment YN (70–118 cm) put TOC, TN, Se, Pb, CaO and Zn into one group (Fig. 5), and these six proxies (bio-elements) showed a similar variation trend (Fig. 4). The PCA analysis results indicated that PC1, characterized by TOC, TN, Se, Pb, CaO and Zn, is the main controlling factor in variations of these element contents. The loadings for PC1 had similar variation trends as bio-elements in YN (Fig. 4) and were significantly correlated with TOC and TN contents ($r=0.90$ and $r=0.89$, respectively); thus, PC1 loadings likely represented the total organic matter contents.

Discussion

Chronology of the 70–118 cm layer

As shown in Table 1, nearly all the radiocarbon dates were older than 13,000 BP and some were as old as ~30,000 BP. Considering the fact that sea level on Broggerhalvøya fell rapidly (30 m kyr^{-1}) after 10,000 BP (Forman et al. 1987) and the time of local deglaciation was ~9440 BP in Spitsbergen (Forman and Miller 1984; Forman et al. 2004), we concluded that the palaeo-notch sediment was influenced by the input of old carbon. Indeed, we detected an unresolved complex matrix (UCM) in the YN sediment (Wang and Sun 2007); UCM is commonly found in soil polluted by petroleum or coal, further confirming the pollution from the Tertiary coal mine in Ny-Ålesund. Thus, radiocarbon dates of the palaeo-notch sediment were not useable for establishing the chronology of the sediment profile YN. The AMS ^{14}C dating results of two selected mollusk shell debris samples from the bottom of the sediment profile (YN-33, YN-34)

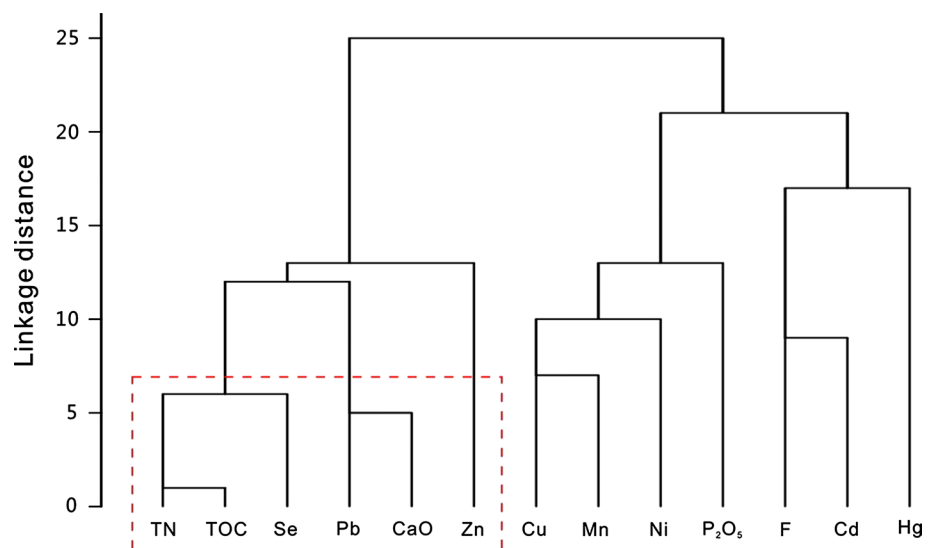
had an average of ~9400 BP (Yuan et al. 2010, 2011). The Kongsfjorden was completely deglaciated by 9440 ± 130 BP (Lehman and Forman 1992; Forman et al. 2004), the elevation of the first terrace in this study was close to the sea level at 9440 BP, and these shells were unlikely transported from a higher terrace. Thus, the mollusk shell debris likely accurately dated the terrace (Yuan et al. 2011), and we considered ~9400 BP as the age of the bottom of YN.

Fortunately, we collected a well-preserved sediment profile, LDP, with precise chronology (Yang et al. 2018a) on Blomstrandhalvøya island (Fig. 1), ~5 km from the sampling site of YN. The close distance between the two sampling sites ensures that the two areas experienced the same climate change and thus the same weathering history. Therefore, we calculated the chemical index of alteration (CIA) of YN according to the formula given by Nesbitt and Young (1982) and compared it with LDP (Yang et al. 2018a). The weathering history of the two sediment profiles showed good agreement with each other; thus, we used the chronology of LDP to correct the chronology of YN based on weathering history (Fig. 6a). We selected seven points (including well-matched peaks and troughs) together with the bottom age to determine the chronology of YN (Fig. 6b), which was further supported by the correlation of TOC contents (Online Resource 1).

Historical photosynthetic biomass production

Organic biomarkers have been used to reconstruct the historical variations of vegetation abundance and penguins in the Antarctic (Wang et al. 2007; Huang et al. 2010). Although application of biomarkers may face the problem of degradation, the cold environment in the Arctic is favorable for the preservation of biomarkers, which can be preserved for thousands of years (Ogura et al. 1990; Cheng et al. 2016),

Fig. 5 R-cluster analysis result for the chemical elements in the palaeo-notch sediment YN



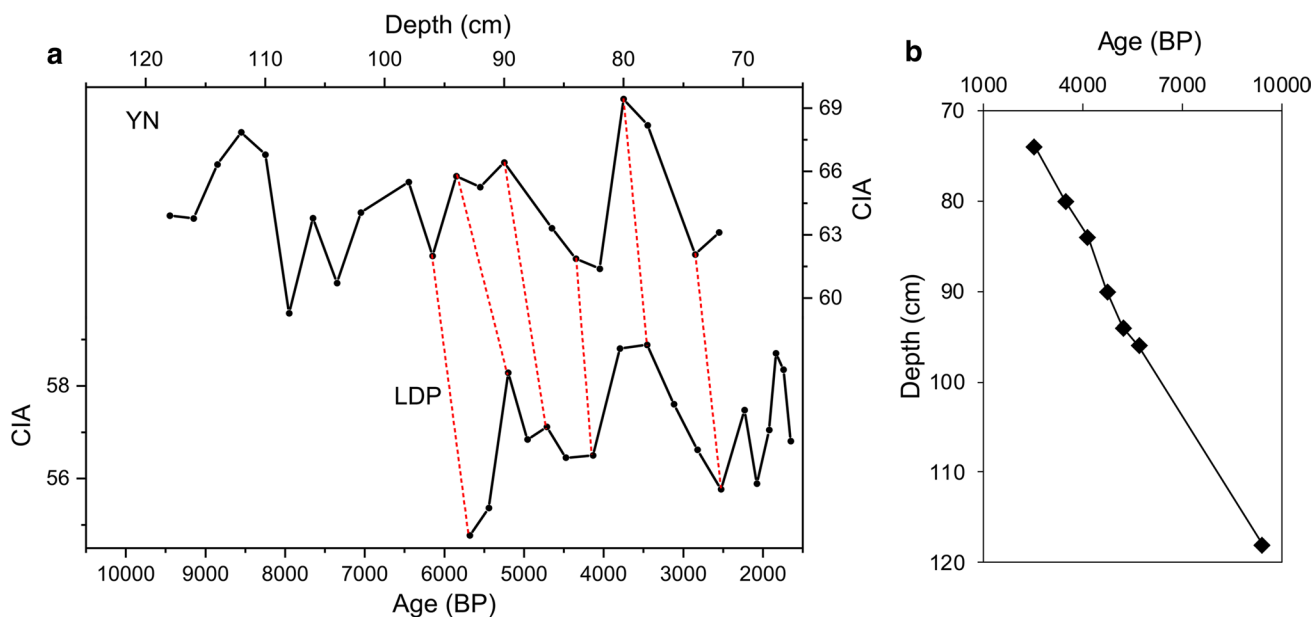


Fig. 6 Comparison of weathering intensity (CIA) between YN and LDP (Yang et al. 2018a) (the red dashed lines indicate the well matched points) (a), and the chronology for the palaeo-notch sediment YN (b). (Color figure online)

and can be an ideal palaeoecological proxy for the reconstruction of the total amount of phytoplankton and terrestrial plants in polar regions.

Among biomarkers, phytol derives from the ester-linked side-chain of chlorophyll-a, which mainly comes from phytoplankton and terrestrial plants (Bechtel and Schubert 2009). Therefore, the concentration of phytol reflects the amount of phytoplankton and terrestrial plants transported to the sediment, and has been used to reflect photosynthetic biomass (Boon et al. 1996) and overall vegetation variations in the Antarctic (Wang et al. 2007; Huang et al. 2010, 2011; Hu et al. 2013). In Svalbard, there is a great diversity of vegetation, and four common tundra plant species (*Dicranum angustum*, *Puccinellia phryganodes*, *Salix polaris* and *Saxifraga oppositifolia*) were found at the sampling site (Yuan et al. 2010). In addition, it has been confirmed that the net primary production in Ny-Ålesund reflects the local photosynthetic capacity and biomass production (Muraoka et al. 2008). Thus, the phytol in YN was very likely derived from the phytoplankton and tundra plants around the palaeo-notch, and its concentration, to a large extent, reflected the photosynthetic biomass production in the study area. In this study, the phytol contents in the palaeo-notch sediment YN from Ny-Ålesund was used to reconstruct photosynthetic biomass production during the interval of 9400–2200 BP (Fig. 3).

The different types of vegetation (Fig. 3) in the palaeo-notch sediment YN was also distinguished according to *n*-alkanol distributions (Meyers 2003; Wang et al. 2007).

As the content of *n*C18-ol was significantly higher than that of *n*C20-ol, we used *n*C18-ol as the proxy of algae. The inputs of lacustrine phytoplankton (*n*C18-ol) and terrestrial plants (*n*C28-ol and *n*C30-ol) exhibited a similar variation trend (Fig. 3), and they were consistent with the reconstructed photosynthetic biomass production.

Inorganic bio-elements have been identified as an important geochemical proxy for the input of specific material sources in the sediment cores. They have been successfully used to reconstruct seabird populations from bird colonies in both the Antarctic (Sun et al. 2000) and the South China Sea (Liu et al. 2006; Xu et al. 2011). According to the results of R-mode cluster and PCA analysis, the loadings for PC1 were significantly correlated with TOC and TN contents and likely represented the total organic matter input. Although the study area is not a seabird colony, input of seabird feces to the sediment profile YN is inevitable. Therefore, the sources of organic matter in YN comprised tundra plants, phytoplankton and seabird feces, and the loadings for PC1 represented the total biomass content. Although it is hard to determine the relative proportions of different organic matter sources, the variations of vegetation, phytoplankton and seabirds are all positively linked to temperature changes in both the Arctic and Antarctic (Birks 1991; Sun et al. 2000, 2004; Yoon et al. 2006; Alsos et al. 2016; Yang et al. 2018b). Therefore, the loadings for PC1 could be used as an auxiliary proxy for photosynthetic biomass.

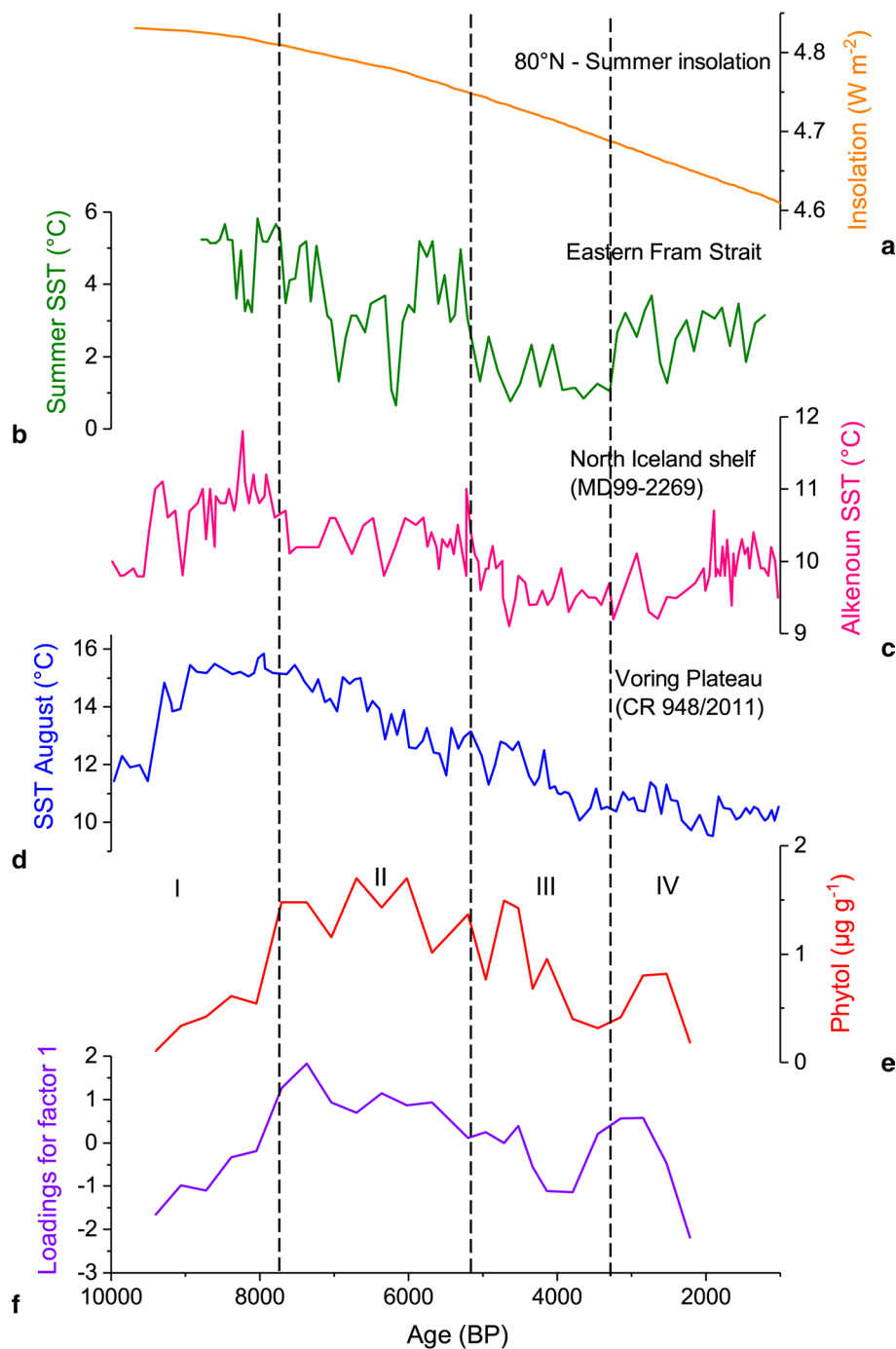
Photosynthetic biomass production and its response to climate change

The reconstructed photosynthetic biomass record in Ny-Ålesund, as indicated by phytol abundance, was consistent with total organic input (PC1) and experienced four periods of different change patterns (Fig. 7e, f). In period I (9400–7700 BP), the photosynthetic biomass production increased steadily. In period II (7700–200 BP), the photosynthetic biomass fluctuated, but stayed at a high level,

likely due to relatively warm temperatures during the Holocene thermal maximum (HTM). In period III (5200–300 BP), there were substantial fluctuations, but in general photosynthetic biomass declined. In period IV (3300–2200 BP), the photosynthetic biomass showed a small peak during the interval of 3000–2500 BP.

In this study, we used the fatty acid $C_{18:2}/C_{18:0}$ ratio as a proxy of palaeotemperature and compared it with our reconstructed photosynthetic biomass (phytol), lacustrine phytoplankton (nC_{18-ol}) and terrestrial plants (nC_{28-ol})

Fig. 7 Comparisons between photosynthetic biomass record in Ny-Ålesund and palaeoclimatic record in the Arctic. **a** Summer insolation at 80°N (Huybers 2006), **b** a SIMMAX-based summer SST reconstruction for the eastern Fram Strait (Werner et al. 2013), **c** an alkenone-based summer SST reconstruction for the North Iceland shelf (Kristjánsdóttir et al. 2017), **d** reconstructed SST for the Voring Plateau (Andersen et al. 2004), **e** reconstructed photosynthetic biomass variations based on phytol in Ny-Ålesund, **f** loadings for factor 1 (PC1) represents the total organic matter input in the palaeo-notch sediment YN



and nC_{30-ol}) record (Fig. 3). Overall, high photosynthetic biomass production corresponded with high temperature except for the initial stage of the record. It may have taken some time for the photosynthetic organisms to establish and develop after deglaciation even though the climate was warm at that time. To explain these substantial variations of photosynthetic biomass production, we also compared the reconstructed photosynthetic biomass with other palaeoclimatic records around Svalbard (Fig. 7).

The photosynthetic biomass was initially at low levels around 9400 BP and then started to rise steadily. The $C_{18:2}/C_{18:0}$ ratios indicated a high temperature during this period, consistent with the high SST records from the North Iceland shelf (Kristjánsson et al. 2017) and Voring Plateau, NE Atlantic (Andersen et al. 2004). In addition, an alkenone-based temperature reconstruction for High Arctic Svalbard indicated that the climate during this period was warmer than the late Holocene (van der Bilt et al. 2016). Therefore, the sustained increase of photosynthetic biomass after 9400 BP is likely linked with the warm climate conditions, which is favorable for the establishment of vegetation and phytoplankton in the study area after deglaciation.

During Period II, the photosynthetic biomass stayed at a relatively high level with a peak around 7700 BP. This period coincides with the HTM in this area; it was very warm and thus favorable for growth of phytoplankton and vegetation. Records from Lake Skartjørna, Svalbard, also revealed highest abundance and diversity of plant macrofossils during 8500–6400 BP (Alsos et al. 2016). Furthermore, the peak of photosynthetic biomass around 7700 BP is consistent with the alkenone-based reconstruction of the temperature maximum around 7800 BP (van der Bilt et al. 2016).

The warm conditions around 7800 BP were mainly driven by strong summer insolation (van der Bilt et al. 2016). In fact, the HTM is not only known from Svalbard during this period but is also observed in many other Arctic regions. The reconstructed SST records from the North Iceland shelf (Kristjánsson et al. 2017), Voring Plateau (Andersen et al. 2004) and eastern Fram Strait (passage between Greenland and Svalbard) (Werner et al. 2013) all indicated relatively warm conditions from 8200 to 5500 BP (Fig. 7b–d), consistent with the palaeotemperature records based on the $C_{18:2}/C_{18:0}$ ratio in this study. In south Greenland, the HTM took place between 8000 and 2000 BP, with the warmest conditions around 7500 BP, while in west Greenland the maximum of water temperature took place between 7000 and 6500 BP (Kaufman et al. 2004). Moreover, the maximum in pollen accumulation rates was observed between 7500 and 6700 BP in Iceland (Kaufman et al. 2004). The warm climate and improved environment during period II likely sustained flourishing vegetation and phytoplankton communities near Ny-Ålesund.

During Period III, the photosynthetic biomass between 5200 and 3300 BP displayed a rapid decrease and large fluctuation. This circumstance was likely associated with the mid-Holocene transition from HTM warming to cooling (Larsen et al. 2012). The reconstructed SST records from the North Iceland shelf, Voring Plateau and eastern Fram Strait all showed a similar rapidly decreasing trend (Fig. 7b–d). A sharp decrease in the overall concentration of plant macrofossils and the richness of sedimentary ancient DNA (*sedaDNA*) from 6000 to 4000 BP has been observed in a lacustrine sediment in Svalbard (Alsos et al. 2016). As shown in Fig. 7e, the decline in photosynthetic biomass at ~5200 BP marked the termination of the HTM, consistent with the drop in biogenic silica and diatom abundance in central Iceland (Larsen et al. 2012). The extremely low level of photosynthetic biomass around 4300 BP was likely related to the “4.2 ka” sudden cooling event, which was recorded from many places in the Arctic (Bond et al. 1997; Larsen et al. 2012; Roland et al. 2014). Van der Knaap (1988) also reported that the wetness of the peat-forming vegetation increased in three phases between 4400 and 2450 BP, possibly due to the climate cooling. The transition to cold conditions was likely related to the gradual weakening summer insolation, representing threshold responses to the strengthening influence of Arctic sea-ice and surface waters (van der Bilt et al. 2016).

During Period IV, the photosynthetic biomass showed a small peak during the period 3000–2500 BP. The variation pattern of this record did not seem to be consistent with the reconstructed SST records from the North Iceland shelf and the Voring Plateau, but was consistent with the summer SST records from the eastern Fram Strait. Thus, regional climate change and environmental conditions likely had a greater impact on photosynthetic biomass production during this period. Low-frequency North Atlantic Oscillation (NAO) may have governed Late Holocene climate variability on Svalbard (van der Bilt et al. 2016). Positive NAO phases are characterized by warm conditions and reduced sea-ice coverage around Svalbard, and negative ones by cold conditions (van der Bilt et al. 2016). The reconstructed NAO index indicated that the climate pattern was dominated by positive NAO phases between 3300 and 2500 BP (Olsen et al. 2012). The relatively warm climate during the period 3300–2500 BP in Ny-Ålesund is further supported by the alkenone-based SST reconstruction for High Arctic Svalbard (van der Bilt et al. 2016).

The good agreement between past photosynthetic biomass in Ny-Ålesund and palaeoclimatic records from the surrounding regions suggests that past photosynthetic biomass production in the Arctic may be mainly driven by temperature. The past photosynthetic biomass increased during warm periods and decreased during cold periods. Similar observations were found from Lake Skartjørna, Svalbard

(Alsos et al. 2016). In addition, several studies have revealed that both plant biomass (Van Der Wal and Stien 2014) and shrub growth (Rozema et al. 2009; Weijers et al. 2010; Buchwal et al. 2013) in Svalbard are positively correlated with summer temperature.

Conclusions

Based on detailed analyzes of organic biomarkers and geochemical proxies, we have reconstructed the photosynthetic biomass record during the interval of 9400–2200 BP in Ny-Ålesund, Svalbard. The photosynthetic biomass apparently experienced four periods over the studied timespan: development (9400–7700 BP), flourishing (7700–5200 BP), fall (5200–300 BP) and fluctuation (3300–2200 BP). Overall, historical photosynthetic biomass change was consistent with temperature variation in the Arctic; the photosynthetic biomass production increased during warmer periods, and vice versa. Therefore, the photosynthetic biomass in the area near Ny-Ålesund may have been controlled by temperature changes over the period 9400–2200 BP.

Acknowledgements The research was supported by Chinese Polar Environment Comprehensive Investigation & Assessment Programmes (CHINARE2017-02-01, CHINARE2017-04-04) and the External Cooperation Program of BIC, CAS (Project No.211134KYBS20130012). Samples provided by the Polar Sediment Repository of Polar Research Institute of China (PRIC). Samples Information and Data were issued by the Resource-sharing Platform of Polar Samples (<https://birds.chinare.org.cn>) maintained by Polar Research Institute of China (PRIC) and Chinese National Arctic & Antarctic Data Center (CN-NADC). We thank the Chinese Arctic and Antarctic Administration and PRIC for logistical support in field. We also thank the Governor of Svalbard for permission to carry out fieldwork.

Compliance with ethical standards

Conflict of interest The authors declare that they have no conflict of interest.

References

- Alsos IG, Sjögren P, Edwards ME, Landvik JY, Gielly L, Forwick M, Coissac E, Brown AG, Jakobsen LV, Føreid MK (2016) Sedimentary ancient DNA from Lake Skartjørna, Svalbard: Assessing the resilience of arctic flora to Holocene climate change. *Holocene* 26:627–642
- Andersen C, Koc N, Jennings A, Andrews J (2004) Nonuniform response of the major surface currents in the Nordic Seas to insolation forcing: implications for the Holocene climate variability. *Paleoceanography*. <https://doi.org/10.1029/2002PA000873>
- Bechtel A, Schubert CJ (2009) A biogeochemical study of sediments from the eutrophic Lake Lugano and the oligotrophic Lake Brienz, Switzerland. *Org Geochem* 40:1100–1114
- Birks HH (1991) Holocene vegetational history and climatic change in west Spitsbergen—plant macrofossils from Skardtjørna, an Arctic lake. *Holocene* 1:209–218
- Bond G, Showers W, Cheseby M, Lotti R, Almasi P, Priore P, Cullen H, Hajdas I, Bonani G (1997) A pervasive millennial-scale cycle in North Atlantic Holocene and glacial climates. *Science* 278:1257–1266
- Boon PI, Virtue P, Nichols PD (1996) Microbial consortia in wetland sediments: a biomarker analysis of the effects of hydrological regime, vegetation and season on benthic microbes. *Mar Freshw Res* 47:27–41
- Buchwal A, Rachlewicz G, Fonti P, Cherubini P, Gärtner H (2013) Temperature modulates intra-plant growth of *Salix polaris* from a high Arctic site (Svalbard). *Polar Biol* 36:1305–1318
- Cheng W, Sun L, Kimpe LE, Mallory ML, Smol JP, Gallant LR, Li J, Blais JM (2016) Sterols and stanols preserved in pond sediments track seabird biovectors in a High Arctic environment. *Environ Sci Technol* 50:9351–9360
- Chistyakova NO, Ivanova EV, Risebrobakken B, Ovsepyan EA, Ovsepyan YS (2010) Reconstruction of the postglacial environments in the southwestern Barents Sea based on foraminiferal assemblages. *Oceanology* 50:573–581
- Cohen J, Screen JA, Furtado JC, Barlow M, Whittleston D, Coumou D, Francis J, Dethloff K, Entekhabi D, Overland J, Jones J (2014) Recent Arctic amplification and extreme mid-latitude weather. *Nat Geosci* 7:627
- Divine D, Isaksson E, Martma T, Meijer HAJ, Moore J, Pohjola V, van de Wal RSW, Godtliobsen F (2011) Thousand years of winter surface air temperature variations in Svalbard and northern Norway reconstructed from ice-core data. *Polar Res* 30:7379
- Førland EJ, Benestad R, Hanssen-Bauer I, Haugen JE, Skaugen TE (2011) Temperature and precipitation development at Svalbard 1900–2100. *Adv Meteorol*. <https://doi.org/10.1155/2011/893790>
- Forman SL, Mann DH, Miller GH (1987) Late Weichselian and Holocene relative sea-level history of Bröggerhalvøya, Spitsbergen. *Quat Res* 27:41–50
- Forman S, Lubinski D, Ingólfsson Ó, Zeeberg J, Snyder J, Siegert M, Matishov G (2004) A review of postglacial emergence on Svalbard, Franz Josef Land and Novaya Zemlya, northern Eurasia. *Quat Sci Rev* 23:1391–1434
- Forman SL, Miller GH (1984) Time-dependent soil morphologies and pedogenic processes on raised beaches, Bröggerhalvøya, Spitsbergen, Svalbard Archipelago. *Arct Alp Res* 16:381–394
- Hu QH, Sun LG, Xie ZQ, Emslie SD, Liu XD (2013) Increase in penguin populations during the Little Ice Age in the Ross Sea. *Antarctica*. *Sci Rep* 3:2472
- Huang J, Sun L, Huang W, Wang X, Wang Y (2010) The ecosystem evolution of penguin colonies in the past 8,500 years on Vestfold Hills, East Antarctica. *Polar Biol* 33:1399–1406
- Huang J, Sun L, Wang X, Wang Y, Huang T (2011) Ecosystem evolution of seal colony and the influencing factors in the 20th century on Fildes Peninsula, West Antarctica. *J Environ Sci* 23:1431–1436
- Huybers P (2006) Early Pleistocene glacial cycles and the integrated summer insolation forcing. *Science* 313:508–511
- Isaksson E, Hermanson M, Hicks S, Igarashi M, Kamiyama K, Moore J, Motoyama H, Muir D, Pohjola V, Vaikmäe R, van de Wal RSW, Watanabe O (2003) Ice cores from Svalbard—useful archives of past climate and pollution history. *Phys Chem Earth* 28:1217–1228
- Jessen SP, Rasmussen TL, Nielsen T, Solheim A (2010) A new Late Weichselian and Holocene marine chronology for the western Svalbard slope 30,000–0 cal years BP. *Quat Sci Rev* 29:1301–1312
- Kaufman DS, Ager TA, Anderson NJ, Anderson PM, Andrews JT, Bartlein PJ, Brubaker LB, Coats LL, Cwynar LC, Duvall ML

- (2004) Holocene thermal maximum in the western Arctic (0–180 W). *Quat Sci Rev* 23:529–560
- Kawamura K, Ishiwatari R (1981) Polyunsaturated fatty acids in a lacustrine sediment as a possible indicator of paleoclimate. *Geochim Cosmochim Acta* 45:149–155
- Kristjánisdóttir GB, Moros M, Andrews JT, Jennings AE (2017) Holocene Mg/Ca, alkenones, and light stable isotope measurements on the outer North Iceland shelf (MD99-2269): a comparison with other multi-proxy data and sub-division of the Holocene. *Holocene* 27:52–62
- Landvik JY, Bondevik S, Elverhøi A, Fjeldskaar W, Mangerud J, Salvigsen O, Siegert MJ, Svendsen J-I, Vorren TO (1998) The last glacial maximum of Svalbard and the Barents Sea area: ice sheet extent and configuration. *Quat Sci Rev* 17:43–75
- Larsen DJ, Miller GH, Geirsdóttir Á, Ólafsdóttir S (2012) Non-linear Holocene climate evolution in the North Atlantic: a high-resolution, multi-proxy record of glacier activity and environmental change from Hvítárvatn, central Iceland. *Quat Sci Rev* 39:14–25
- Lehman SJ, Forman SL (1992) Late Weichselian glacier retreat in Kongsfjorden, west Spitsbergen, Svalbard. *Quat Res* 37:139–154
- Liu X, Sun L, Xie Z, Yin X, Wang Y (2005) A 1300-year record of penguin populations at Ardley Island in the Antarctic, as deduced from the geochemical data in the ornithogenic lake sediments. *Arct Antarct Alp Res* 37:490–498
- Liu X, Zhao S, Sun L, Luo H, Yin X, Xie Z, Wang Y, Liu K, Wu X, Ding X (2006) Geochemical evidence for the variation of historical seabird population on Dongdao Island of the South China Sea. *J Paleolimnol* 36:259–279
- Mangerud J, Bolstad M, Elgersma A, Helliksen D, Landvik JY, Lønne I, Lycke AK, Salvigsen O, Sandahl T, Svendsen JI (1992) The last glacial maximum on Spitsbergen, Svalbard. *Quat Res* 38:1–31
- Meyers PA (2003) Applications of organic geochemistry to paleolimnological reconstructions: a summary of examples from the Laurentian Great Lakes. *Org Geochem* 34:261–289
- Müller J, Werner K, Stein R, Fahl K, Moros M, Jansen E (2012) Holocene cooling culminates in sea ice oscillations in Fram Strait. *Quat Sci Rev* 47:1–14
- Muraoka H, Noda H, Uchida M, Ohtsuka T, Koizumi H, Nakatsubo T (2008) Photosynthetic characteristics and biomass distribution of the dominant vascular plant species in a high Arctic tundra ecosystem, Ny-Ålesund, Svalbard: implications for their role in ecosystem carbon gain. *J Plant Res* 121:137
- Nesbitt H, Young G (1982) Early Proterozoic climates and plate motions inferred from major element chemistry of lutites. *Nature* 299:715–717
- Ogura K, Machihara T, Takada H (1990) Diagenesis of biomarkers in Biwa Lake sediments over 1 million years. *Org Geochem* 16:805–813
- Olsen J, Anderson NJ, Knudsen MF (2012) Variability of the North Atlantic Oscillation over the past 5,200 years. *Nat Geosci* 5:808–812
- Rasmussen TL, Thomsen E, Skirbekk K, Ślubowska-Woldengen M, Kristensen DK, Koç N (2014) Spatial and temporal distribution of Holocene temperature maxima in the northern Nordic seas: interplay of Atlantic-, Arctic- and polar water masses. *Quat Sci Rev* 92:280–291
- Reimer PJ, Bard E, Bayliss A, Beck JW, Blackwell PG, Ramsey CB, Buck CE, Cheng H, Edwards RL, Friedrich M, Grootes PM, Guilderson TP, Hafliðason H, Hajdas I, Hatte C, Heaton TJ, Hoffmann DL, Hogg AG, Hughen KA, Kaiser KF, Kromer B, Manning SW, Niu M, Reimer RW, Richards DA, Scott EM, Southon JR, Staff RA, Turney CSM, van der Plicht J (2013) Intcal13 and Marine13 radiocarbon age calibration curves 0–50,000 years cal BP. *Radiocarbon* 55:1869–1887
- Reusche M, Winsor K, Carlson AE, Marcott SA, Rood DH, Novak A, Roof S, Retelle M, Werner A, Caffee M (2014) 10 Be surface exposure ages on the late-Pleistocene and Holocene history of Linnébreen on Svalbard. *Quat Sci Rev* 89:5–12
- Risebrobakken B, Moros M, Ivanova EV, Chistyakova N, Rosenberg R (2010) Climate and oceanographic variability in the SW Barents Sea during the Holocene. *Holocene* 20:609–621
- Roland TP, Caseldine CJ, Charman DJ, Turney CSM, Amesbury MJ (2014) Was there a ‘4.2 ka event’ in Great Britain and Ireland? Evidence from the peatland record. *Quat Sci Rev* 83:11–27
- Rontani JF, Volkman JK (2003) Phytol degradation products as biogeochemical tracers in aquatic environments. *Org Geochem* 34:1–35
- Røthe TO, Bakke J, Vasskog K, Gjerde M, D’Andrea WJ, Bradley RS (2015) Arctic Holocene glacier fluctuations reconstructed from lake sediments at Mitrahallvøya, Spitsbergen. *Quat Sci Rev* 109:111–125
- Rozema J, Boelen P, Doorenbosch M, Bohncke S, Blokker P, Boekel C, Broekman R, Konert M (2006) A vegetation, climate and environment reconstruction based on palynological analyses of high arctic tundra peat cores (5000–6000 years BP) from Svalbard. *Plant Ecol* 182:155–173
- Rozema J, Weijers S, Broekman R, Blokker P, Buizer B, Werleman C, El Yaqine H, Hoogedoorn H, Fuertes MM, Cooper E (2009) Annual growth of *Cassiope tetragona* as a proxy for Arctic climate: developing correlative and experimental transfer functions to reconstruct past summer temperature on a millennial time scale. *Glob Change Biol* 15:1703–1715
- Sun L, Xie Z, Zhao J (2000) A 3000-year record of penguin populations. *Nature* 407:858–858
- Sun L, Liu X, Yin X, Zhu R, Xie Z, Wang Y (2004) A 1,500-year record of Antarctic seal populations in response to climate change. *Polar Biol* 27:495–501
- Svendsen JI, Elverhøi A, Mangerud J (1996) The retreat of the Barents Sea Ice Sheet on the western Svalbard margin. *Boreas* 25:244–256
- van der Bilt WGM, Bakke J, Vasskog K, D’Andrea WJ, Bradley RS, Ólafsdóttir S (2015) Reconstruction of glacier variability from lake sediments reveals dynamic Holocene climate in Svalbard. *Quat Sci Rev* 126:201–218
- van der Bilt WG, D’Andrea WJ, Bakke J, Balascio NL, Werner JP, Gjerde M, Bradley RS (2016) Alkenone-based reconstructions reveal four-phase Holocene temperature evolution for High Arctic Svalbard. *Quat Sci Rev* 183:204–213
- Van der Knaap W (1988) A pollen diagram from Brøggerhalvøya, Spitsbergen: changes in vegetation and environment from ca. 4400 to ca. 800 BP. *Arct Alp Res* 20:106–116
- Van Der Wal R, Stien A (2014) High-arctic plants like it hot: a long-term investigation of between-year variability in plant biomass. *Ecology* 95:3414–3427
- Walker DA, Reynolds MK, Daniëls FJ, Einarsson E, Elvebakk A, Gould WA, Katenin AE, Kholod SS, Markon CJ, Melnikov ES (2005) The circumpolar Arctic vegetation map. *J Veg Sci* 16:267–282
- Wang J, Wang Y, Wang X, Sun L (2007) Penguins and vegetations on Ardley Island, Antarctica: evolution in the past 2,400 years. *Polar Biol* 30:1475–1481
- Wang J, Sun L (2007) Molecular organic geochemistry of ornithogenic sediment from Svalbard, Arctic. *Chin J Pol Sci* 20:32–39
- Weijers S, Broekman R, Rozema J (2010) Dendrochronology in the High Arctic: July air temperatures reconstructed from annual shoot length growth of the circumpolar dwarf shrub *Cassiope tetragona*. *Quat Sci Rev* 29:3831–3842
- Werner K, Spielhagen RF, Bauch D, Hass HC, Kandiano E (2013) Atlantic water advection versus sea-ice advances in the eastern Fram Strait during the last 9 ka: multiproxy evidence for a two-phase Holocene. *Paleoceanography* 28:283–295
- Werner K, Müller J, Husum K, Spielhagen RF, Kandiano ES, Polyak L (2016) Holocene sea subsurface and surface water masses in the

- Fram Strait—Comparisons of temperature and sea-ice reconstructions. *Quat Sci Rev* 147:194–209
- Xu L, Liu X, Sun L, Yan H, Liu Y, Luo Y, Huang J (2011) A 2200-year record of seabird population on Ganquan Island, South China Sea. *Acta Geol Sin* 85:957–967
- Yang Z, Yuan L, Wang Y, Sun L (2017) Holocene climate change and anthropogenic activity records in Svalbard: a unique perspective based on Chinese research from Ny-Ålesund. *Adv Polar Sci* 28:81–90
- Yang Z, Sun L, Zhou X, Wang Y (2018a) Mid-to-late Holocene climate change record in palaeo-notch sediment from London Island, Svalbard. *J Earth Syst Sci* 127:57
- Yang Z, Wang Y, Sun L (2018b) Records in palaeo-notch sediment: changes in palaeoproductivity and their link to climate change from Svalbard. *Adv Polar Sci* 29:243–253
- Yoon H, Khim B, Lee K, Park Y, Yoo K (2006) Reconstruction of postglacial paleoproductivity in Long Lake, King George Island, West Antarctica. *Pol Polar Res* 27:189–206
- Yuan L, Sun L, Long N, Xie Z, Wang Y, Liu X (2010) Seabirds colonized Ny-Ålesund, Svalbard, Arctic ~ 9400 years ago. *Polar Biol* 33:683–691
- Yuan L, Sun L, Wei G, Long N, Xie Z, Wang Y (2011) 9400 yr BP: the mortality of mollusk shell (*Mya truncata*) at high Arctic is associated with a sudden cooling event. *Environ Earth Sci* 63:1385–1393

Publisher's Note Springer Nature remains neutral with regard to jurisdictional claims in published maps and institutional affiliations.